RECONSTRUCTING SOLAR FLARE EFFECTS ON VLF SIGNAL PROPAGATION

J. P. Velásquez[1], **J. Samanés**[1] and **E. Rojas**[2]

[1]National Commission for Aerospace Research and Development (CONIDA), Peru
[2]Haystack Observatory, Massachusetts Institute of Technology

VLF signal propagation in the D-region with LMP

The Earth's surface and the ionosphere act as a natural waveguide for VLF (wavelenghts $\sim$ 10 km - 100 km) signal propagation in the lower ionosphere. Hence, a suitable approach is provided by Mode Theory, which takes advantage of the waveguide eigenmode formulation to propagate the electromagnetic fields throughout the waveguide.

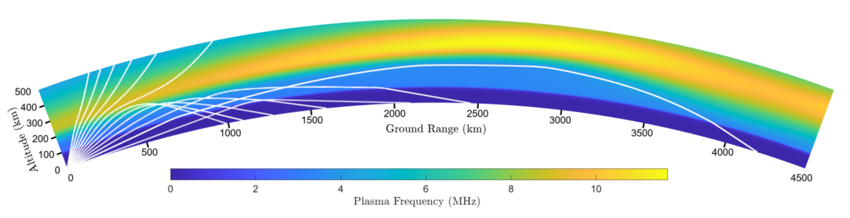

Fig. 1: Geometrical optics picture of signal propagation as given by PHaRLAP[1].

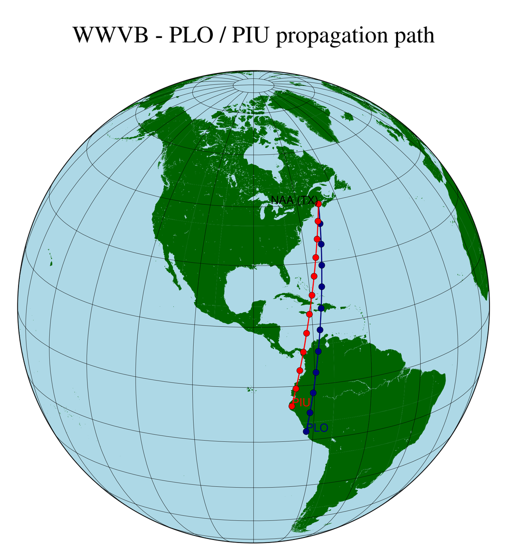

Fig. 2: Links NAA-PLO and NAA-PIU from the SAVNET network [2].

Inversion Framework

Two separate optimization steps were taken: the first one to estimate the background ionosphere density and the second one to find the solar flare-induced density perturbation amplitude parameter.

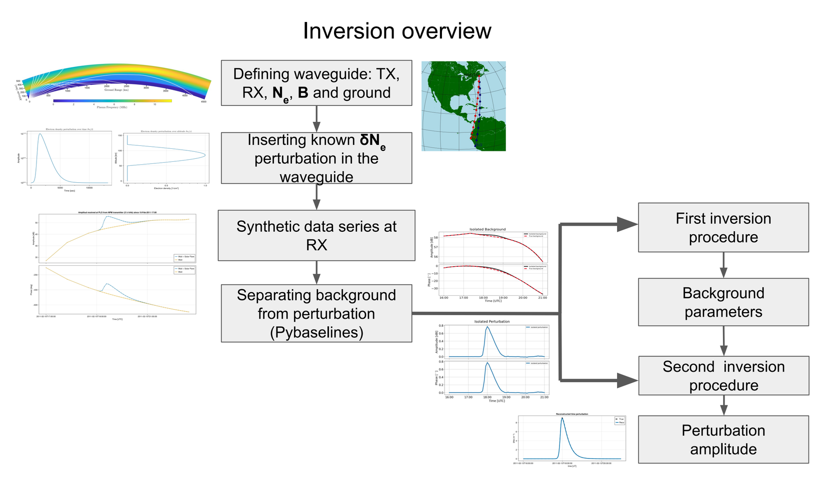

Fig. 3: Flux diagram of the algorithm developed to retrieve solar flare-induced density perturbation parameters.

Solar Flare Effects on VLF signal propagation

A 5 segment-waveguide. N_e given by the Wait&Spies model ([3]), where h and β are parametrized polynomials of the solar zenith angle χ. The solar flare-induced electron density perturbation (δN_e) is described by the product of 2 time sigmoid functions (Figures 4 and 5).

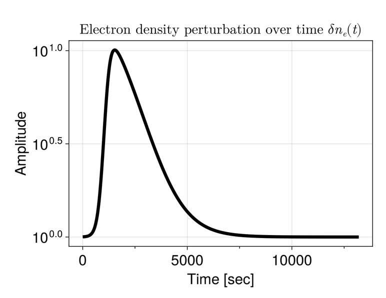

Fig. 4: Time perturbation due to a solar flare.

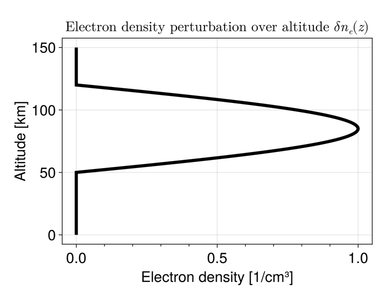

Fig. 5: Altitude profile perturbation due to a solar flare.

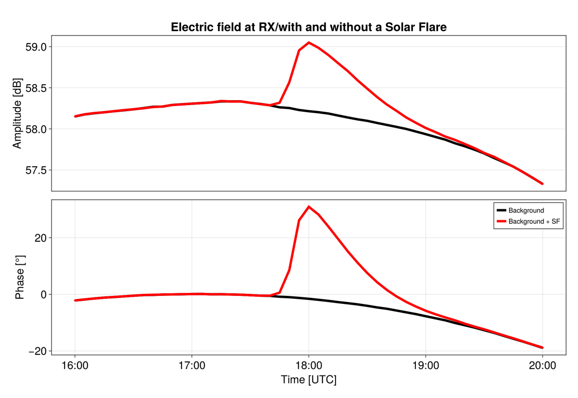

Fig. 6: Magnitude and phase of the electric field detected at the RX station.

Background and perturbation signal separation

The Python package *Pybaselines* [4] was used to separate the signal associated with a quiet ionosphere (Figure 7) from the solar-flare-induced signal (Figure 8).

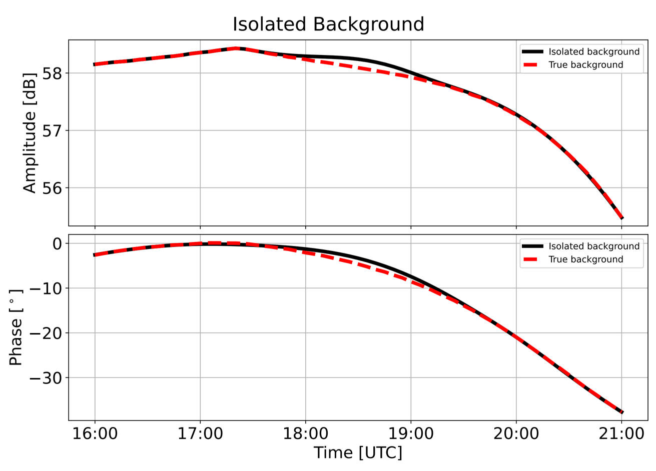

Fig. 7: Isolated background signal associated with a quiet ionosphere.

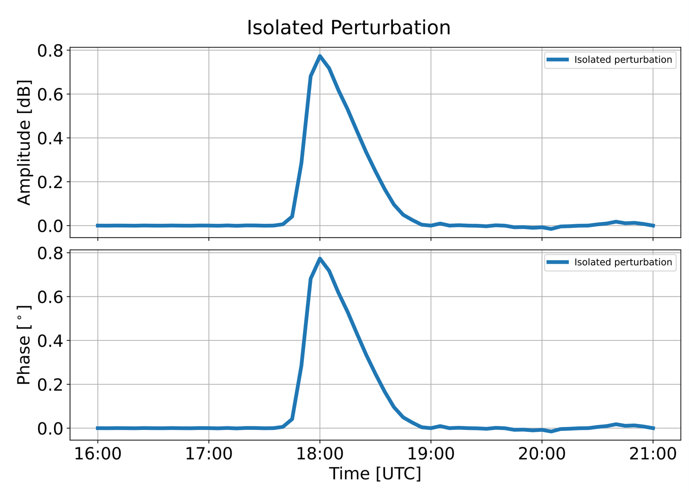

Fig. 8: Isolated perturbation induced by a solar flare.

Simulation-based reconstruction

The first inversion procedure consisted of introducing the isolated background signal to an optimizer and fitting it to a polynomial of the solar zenith angle forward model to obtain the polynomial coefficients. The *BlackBoxOptim* package [5] was utilized to achieve this goal.

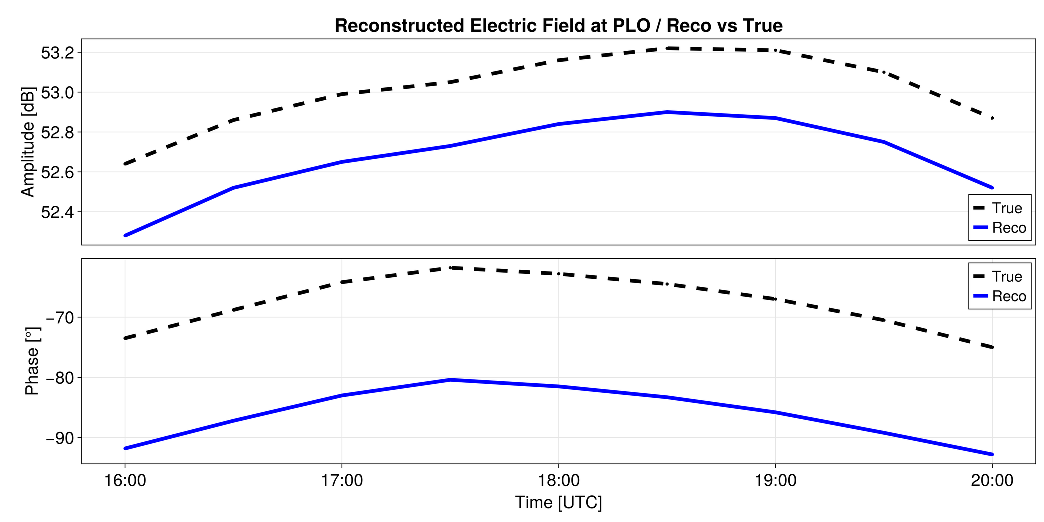

Fig. 9: Reconstructed vs true density enhancement.

The isolated perturbation signal was introduced in a second inversion procedure where the perturbation forward model was represented by a product of 2 sigmoid functions. The reconstructed vs true density perturbation is shown in Figure 10

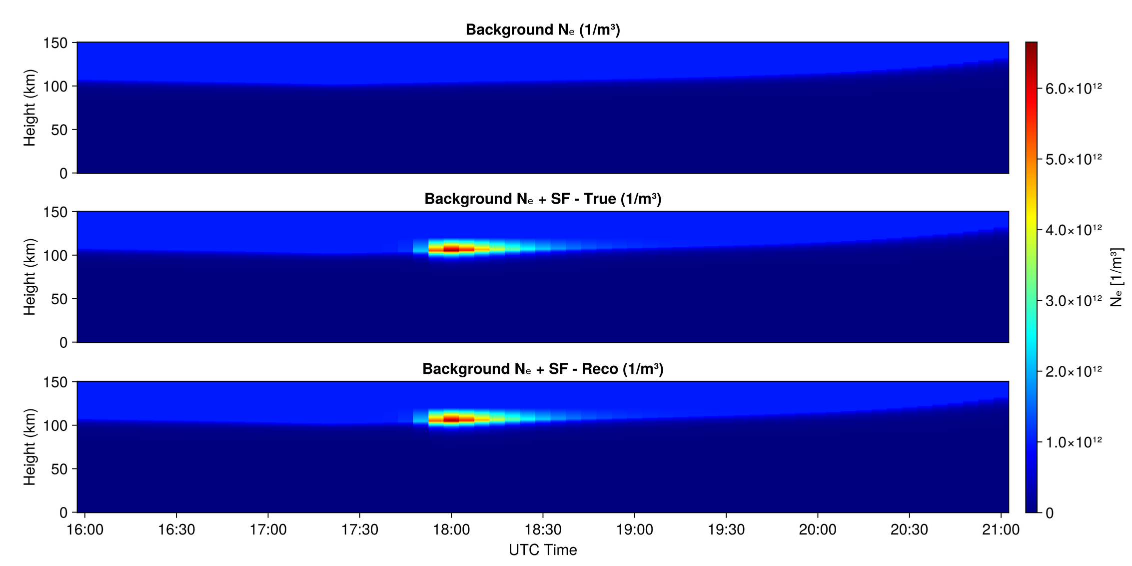

Fig. 10: Reconstructed vs true density enhancement.

Reconstruction on Real Data (I)

The previously explained inversion framework developed with synthetic data was applied to real data corresponding to the occurence of a M1.7 class solar flare on 2008 March 25th. (Figure 11)

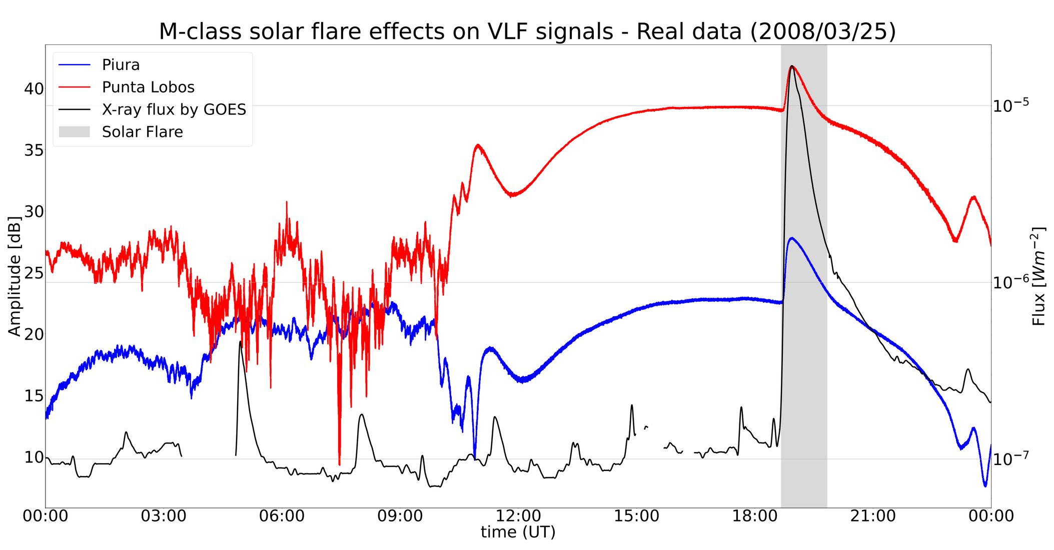

Fig. 11: Amplitude of the total electric field measured at Piura and Punta Lobos RX stations during the 2008 March 25th M-class solar flare occurrence.

Reconstruction on Real Data (II)

The same simulation-based filtering scheme was applied on real data as shown in Figure 12. The obtained isolated background was introduced in a first inversion procedure from which the background polynomial coefficients are estimated. The reconstructed background signal is shown in Figure 13.

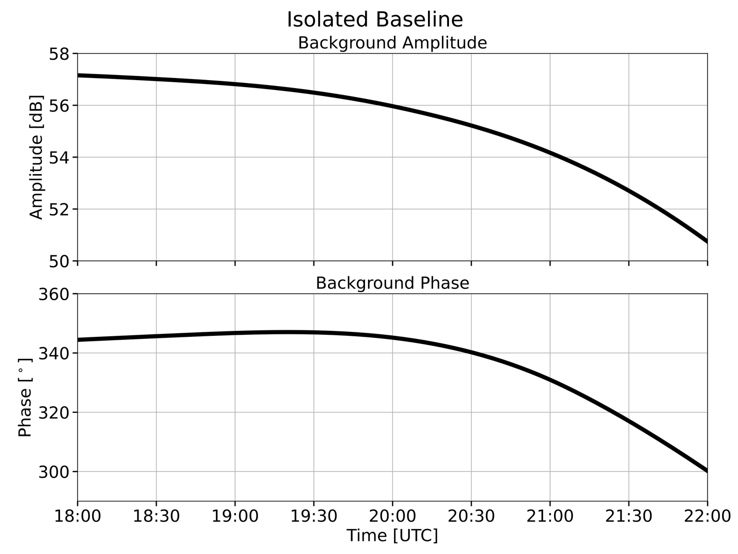

Fig. 12: Real data background signal isolation.

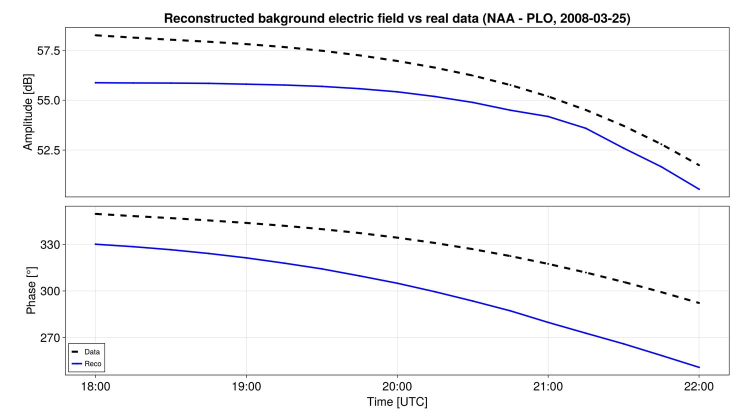

Fig. 13: Reconstructed background signal vs isolated background signal.

Remarks

- The two step simulation-based inversion procedure presented in this work allowed us to decently retrieve the background ionosphere parameters and the perturbation amplitude.
- Preliminary results showed that the developed inversion framework works on real data too (background). The perturbation amplitude estimation is pending.

Acknowledgements

This work has been supported by CONCYTEC through its PROCIENCIA program in the framework of the "Basic Research Projects 2023-01" contest, according to contract No. PE501082050-2023-PROCIENCIA. The authors would like to thank the National Commission for Aerospace Research and Development (Peruvian Space Agency), for its support.

References

[1] *PHaRLAP - Provision of High-frequency Raytracing Laboratory for Propagation studies | DST.* https://www.dst.defence.gov.au/our-technologies/pharlap-provision-high-frequency-raytracing-laboratory-propagation-studies. (Accessed on 11/06/2024).

[2] Jean-Pierre Raulin et al. "The South America VLF NETwork (SAVNET)". In: *Earth, Moon, and Planets* 104 (2009), pp. 247–261. DOI: 10.1007/s11038-008-9269-4.

[3] National Institute of Standards and Commerce Department Technology (NIST). "Characteristics of the Earth-Ionosphere Waveguide for Vlf Radio Waves". In: *Commerce Department* (Jan. 1964). URL: https://www.govinfo.gov/app/details/GOVPUB-C13-1fc83a916d87542f34917847f89b9f0b.

[4] Donald Erb. *pybaselines: A Python library of algorithms for the baseline correction of experimental data.* 2024. DOI: 10.5281/zenodo.5608581. URL: https://github.com/derb12/pybaselines.

[5] Robert Feldt. *BlackBoxOptim.jl: Black-box optimization for Julia.* GitHub repository. Accessed: 2025-06-19. 2025. URL: https://github.com/robertfeldt/BlackBoxOptim.jl.